Structural Investigation of Polyamide-6 and Polyamide-6 Composites Using ^{13}C Cross Polarization/Magic Angle Spinning NMR

T. L. Weeding and W. S. Veeman*

Department of Molecular Spectroscopy, Faculty of Science, University of Nijmegen, Toernooiveld, 6525 ED Nijmegen, The Netherlands

H. Angad Gaur and W. G. B. Huysmans

AKZO Research Arnhem, Corporate Research Department, PO 60, 6800 AB Arnhem, The Netherlands. *Received March 30, 1987*

ABSTRACT: Natural-abundance ^{13}C NMR spectra of pure polyamide-6 (PA6) and polyamide-6 composites were measured with CP and MAS techniques. The microcomposites were made by adding glass microspheres, a silane coupling agent, or prefunctionalized glass spheres to PA6. ^{13}C NMR spectra of these samples show the presence of three components: two crystalline phases and an amorphous component. The chemical shifts of both carbons adjacent to the amide group are sensitive to the PA6 crystal structure; in the dominant α polymorph, C1 and C5 are 3 ppm downfield from their chemical shift values in the γ polymorph. Both the X-ray diffraction powder patterns and the ^{13}C NMR spectra show a change in the relative amounts of the two crystalline components when the composites are made.

Introduction

An important advantage of ^{13}C solid-state NMR spectroscopy of polymers relative to high-resolution ^{13}C NMR studies of polymer solutions is the ability to characterize the conformations that are present in the solid state. Cross polarization (CP), magic angle spinning (MAS), and high-power proton decoupling enable the acquisition of well-resolved ^{13}C NMR spectra in solid polymers with good sensitivity and high resolution. Polyamide-6 (PA6) (or poly(imino(1-oxo-1,6-hexanediyl))) is an industrially important polymer that has received little attention from solid-state ^{13}C NMR spectroscopists. It has, however, been the subject of numerous solution studies, including ^{1}H, ^{13}C, and ^{15}N NMR.[1-3] Broad-line ^{1}H NMR investigations have also been pursued.[4] Similarly, several reports have been made on the structures of PA6 crystals based on X-ray diffraction measurements.[5-9] Polyamide-6 commonly crystallizes in α and γ forms. The α form is the most common and thermodynamically the most stable. In some cases drawing or chemical treatment induce the reversible transformation of α-PA6 into γ-PA6.[9]

The crystal structures of α-PA6 and γ-PA6 are very similar to one another. In both cases the polymer chains are extended along the monoclinic (*b*) axis. The chain directions, which are defined by the orientation of the carbonyl and amino groups, alternate along the direction of the *a* axis and are parallel along the *c* axis. The hydrogen bonding in the α polymorph is between antiparallel adjacent chains, and in the γ polymorph hydrogen bonding is between parallel chains. In the γ-PA6 crystal the amide linkage is rotated by approximately 60° relative to the plane of the methylene chain, whereas the amide linkage lies in the plane of the methylene chain in α-PA6. The hydrogen bonds are 2.81 Å in α-PA6 and 2.83 Å in γ-PA6. The unit cell of α-PA6 is 2% longer along the chain axis than the unit cell of γ-PA6, but the density of α-PA6 is about 6% greater than the density of γ-PA6. These subtle changes in polymer conformation are easily observed in the ^{13}C CP/MAS spectra.

As the mechanical properties of many polymers may be profitably modified by adding other components such as cross-linking agents, inorganic fillers, or other polymers, the characterization of possible structural changes in the host macromolecule are of interest. Here we report an investigation of PA6 and PA6 composites containing glass microspheres, a silane coupling agent, or prefunctionalized glass spheres using the techniques of ^{13}C MAS NMR and X-ray diffraction.

Experimental Section

Samples. The PA6 and PA6 composites were prepared at AKZO (Arnhem, The Netherlands). The polymer was a commercial product with a relative viscosity of 2.37 in 1% formic acid solution. Glass microspheres of mean diameter 50.0 μm, a silane coupling agent ((3-aminopropyl)triethoxysilane), or the same glass balls prefunctionalized with the coupling agent were added by using a single-screw extruder. The final temperature reached in the extruder was 260 °C, well above the melting temperature (210 °C). After leaving the extruder, the materials were cooled within 1 s. Five samples were studied, all from the same original batch of PA6. Sample 1 was pure PA6, sample 2 was PA6 with glass balls (30% by weight), sample 3 was PA6 with silane coupling agent (1% by weight), sample 4 was PA6 with prefunctionalized glass balls (30% by weight in the composite, 1% coupling agent on the balls), and sample 5 was PA6 freshly extruded without any additives. Samples 1–4 were aged for 3 years under ambient conditions before use in these experiments, and sample 5 was studied soon after extrusion and during the year and a half following its preparation.

NMR Spectroscopy. The NMR data for the composites were acquired at room temperature on a Bruker CXP 300 (7.0 T) spectrometer operating at 75.4 MHz with a Bruker double-bearing CP/MAS probe. The spectra of the PA6 fibers were collected on a Bruker CXP 200 (4.7 T) operating at 50.3 MHz. Chemical shifts were referenced to an external standard of adamantane, methylene resonance at 38.56 ppm[10] relative to TMS. Typical CP pulse sequences used a 3.5–4.5 μs 90° pulse, 1-ms mixing time, and a 2-s recycle time, collecting 1024 points in the time domain for a 25-kHz spectral width. Phase cycling and spin temperature alternation were included to minimize artifacts.[11] Samples were spun at the magic angle at 3.5–4.5 kHz by using compressed air.

The spectra of the amorphous fractions of these samples were measured by using 90° pulses at 1-s intervals, high-power proton decoupling, and MAS.

X-ray Diffraction. The WAXS (wide-angle X-ray scattering) measurements were made with a Philips PW 1050 automatic diffractometer equipped with a focusing graphite monochromator. Cu Kα radiation was used in the symmetric diffraction technique. The 2θ range was scanned between 5° and 50° in increments of 0.025°. At each 2θ position, counts were collected for 20–30 s.

The WAXS patterns obtained for the extrudates severely overlap. A computer program,[8] which had been developed to resolve the diffraction patterns of PA6 fibers into five components derived from the α and γ crystalline phases and the amorphous phase, was employed to try to quantify these data. In the original program, developed for axially symmetric fibers, a coupling between the two diffraction peaks of both the α and the γ crystallites

0024-9297/88/2221-2028$01.50/0

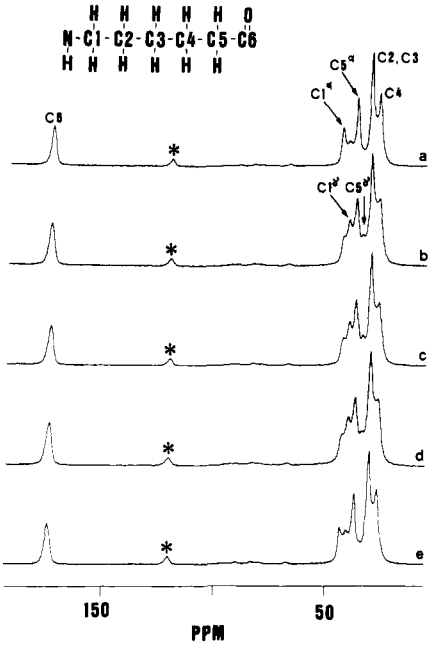

Figure 1. ^{13}C CP/MAS spectra of the five PA6 and PA6 composite samples. The asterisk indicates spinning side bands. Chemical shift values are listed in table I. The magic angle spinning rate was 4 kHz, mixing time 1 ms, and recycle delay 2 s. Data were collected at 75 MHz: (a) sample 1, PA6, 5000 FIDs; (b) sample 2, PA6 with glass balls, 6900 FIDs; (c) sample 3, PA6 with silane coupling agent, 7000 FIDs; (d) sample 4, PA6 with prefunctionalized glass balls, 5400 FIDs; (e) sample 5, PA6 soon after extrusion, without any additives, 4200 FIDs.

was possible due to fiber symmetry. In the case of extrudates, which have no axial symmetry, this restriction had to be deleted. Unfortunately this resulted in too many parameters for these poorly resolved diffraction patterns, and quantitative analysis was therefore unsuccessful.

Results and Discussion

MAS NMR Spectroscopy. Figure 1 shows a comparison between the CP/MAS spectra of the original PA6, sample 1, the three composite samples, samples 2–4, and sample 5, which was processed by the same extrusion process but without the addition of any other components. In Figure 1a, the downfield resonance at 173.4 ppm comes from the only nonaliphatic carbon, C6, the carbonyl carbon. Comparison of the chemical shifts observed in this spectrum with those of PA6 in $HFSO_3$ solution[2] and those predicted by addivity rules[12] enables the assignment of the aliphatic peak at 42.8 ppm to C1, at 30.1 ppm to C2 and C3, at 26.5 ppm to C4, and at 36.8 ppm to C5. The CP/MAS spectra are a superposition of the spectra of the crystalline and the amorphous material. However, the narrower line widths of the crystalline fraction cause it to dominate the CP/MAS spectrum, and the lines assigned here are therefore essentially due to the crystalline fraction.

The carbonyl resonance position and the positions of some of the aliphatic resonances are unaffected by the processing. However, in samples 2–4, (Figures 1b–d, respectively) two new peaks appear at 40 and 34 ppm, while the intensity at 43 ppm has significantly decreased as has, less clearly, the intensity at 37 ppm. We first confirmed that the new resonances were due to other conformations and not to ^{14}N quadrupole effects by examining the samples at higher (9.4 and 11.7 T) and lower, (4.7 T) magnetic fields. No changes in the peak positions were observed. We then compared the spectra with the ^{13}C CP/MAS spectra of two PA6 fiber samples that were known from X-ray diffraction analysis[9] to contain, in the first case

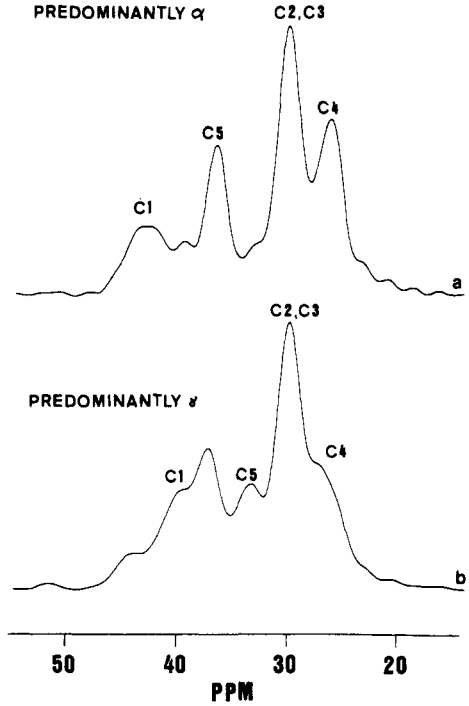

Figure 2. ^{13}C CP/MAS spectra of the aliphatic regions of samples of PA6 yarns. Data were collected at 50 MHz: (a) sample containing predominantly α-PA6; (b) sample containing predominantly γ-PA6.

Table I
^{13}C Chemical Shifts[a] in PA6/PA6 Composites

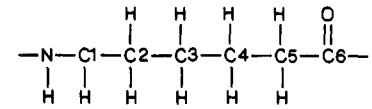

sample	carbon C1	C2	C3	C4	C5	C6
PA6/PA6 composites						
α form	42.8	30.1	30.1	26.5	36.8	173.4
γ form	39.9	30.0	30.0	26.7	33.9	173.4
amorphous	40.1	29.8	27.9	26.2	36.3	173.4
fibers						
predominantly α-PA6	42.6	30.0	30.0	26.0	36.4	173.4
predominantly γ-PA6	39.9	29.8	29.8	26.4	33.6	173.4
solution[b]	43.5	26.6	25.3	24.3	33.5	179.3

[a] In ppm relative to TMS. [b] From ref 2; C2, C3, and C4 resonances were not individually assigned by the authors.

(spun at 500 m/min) predominantly α-PA6 crystallites, and in the second case (spun at 6000 m/min) predominantly γ-PA6 crystallites. These spectra are shown in Figure 2, parts a and b, respectively. The similarity of the chemical shifts observed for the yarn samples known to contain predominantly α- or γ-PA6 crystallites with the chemical shifts for the composites indicates the presence of α-like and γ-like PA6 structures in the extrudates. We will refer to these PA6 structures as α-PA6 and γ-PA6 throughout the remainder of this paper.

The peaks at 42.8 and 36.8 ppm are assigned to C1 and C5 in the α polymorph, respectively, and the peaks at 39.9 and 33.9 ppm to C1 and C5 in the γ polymorph, respectively. Although the resonances corresponding to the carbonyl carbon, C6, and carbons C2 and C3 have the same chemical shift values in both crystalline phases, C4 in the α polymorph is found about 0.5 ppm upfield from its value in the γ polymorph. This chemical shift difference for C4 results in decreased resolution of the peaks at 30.1 and 26.5 ppm in the composites. Peak assignments are given in

Table I. The 3-ppm difference between the ^{13}C chemical shifts for C1 and C5 in these two crystalline forms is comparable to the difference in chemical shifts observed for the α carbon in the α-helix and β-pleated sheet structures of polypeptides, e.g., 3.5 ppm for poly-L-alanine.[13]

As has been observed for other polymer systems,[14-17] the carbons in the amorphous fraction of these samples have much shorter spin–lattice relaxation times, T_1, than do the carbons in the crystalline fraction. The T_1 values of the aliphatic carbons in the crystalline part of these PA6 composite samples were found to be 10–20 s. The aliphatic carbons in the amorphous part had T_1 values of 0.5–0.75 s. The carbonyl T_1 values are longer, 40 and 5 s in the crystalline and amorphous fractions, respectively. These spin–lattice relaxation times are about half as long as those in the original untreated PA6 sample. The difference between the T_1 values of the two fractions means that the spectra of the predominantly amorphous fraction can be obtained by the application of closely spaced 90° pulses that saturate the crystalline carbons. The spectra of the amorphous fractions of all five samples are very similar to one another. There is no evidence of resonances originating from the carbons in the coupling agent. The amorphous peaks have widths on the order of 300 Hz (full width at half-height), which are broader than the line widths of the crystalline fraction, which are approximately 100 Hz wide. These resonances of the amorphous carbons are remarkably well resolved compared to those in the amorphous fractions of some other polymers. For example, in poly(3,3-diethyloxetane) the peaks of backbone and side-chain carbons are well resolved in the crystalline fraction, but only one carbon resonance is observed for the four different carbons in the amorphous phase.[18] Due to the overlap of some of the lines in the spectra of the amorphous fractions of these PA6 composites, an analog curve resolver (Du Pont 310) was used to estimate the line positions. In the amorphous phase, C1 is found at 40 ppm, as in the γ crystalline form, C5 is found at 37 ppm, as in the α crystalline form, and C2 and C3 no longer have the same chemical shift value. While no precise assignment of the polymer conformation in the amorphous phase may be made on the basis of these chemical shift values, it is clear that the conformations present in the amorphous phase are not simply an average over the α and γ crystalline structures. Rather, there is significant ordering, and this fraction may be more appropriately called noncrystalline than amorphous. Illers and Haberkorn[19] have reported specific-volume data that indicated that there were two types of amorphous regions in PA6, which depended upon the crystalline polymorph present in greatest abundance; we are able to detect only one type of amorphous environment with NMR. In view of the observed values of the chemical shifts of C1 and C5, it seems questionable whether one can ascribe any specifically α or γ character to the amorphous phase. Curiously, the chemical shifts of C1 and C5 in $HFSO_3$ solution show the opposite behavior: C1 is found at 43.5 ppm (α-like), and C5 at 33.5 ppm (γ-like).

To test whether the process of extrusion affected the amount of γ-PA6, which was present in only small amounts in the original sample, we prepared a new sample, sample 5, by processing PA6 under the same conditions but without any additives. This resulted in an enhancement of the resonance at 40 ppm. Although it overlaps with the amorphous peak at 40 ppm, this enhancement indicates an increase in the amount of γ-PA6 in sample 5 relative to sample 1, but not as much as that which was found to be present in the composite samples 2–4 (see Figure 1e). The process of extrusion alone apparently enhances the formation of γ crystallites in the extrudates. However, the increased relative amount of γ-PA6 is not stable over time. The CP/MAS spectrum of sample 5 taken over a year after extrusion, shown in Figure 3, showed a decrease in the amount of γ-PA6 consistent with the greater thermodynamic stability of the α polymorph. Therefore, the increased amounts of the γ polymorph in the crystalline fractions of the composites may indicate that the silane coupling agent, the glass balls, and the prefunctionalized glass balls encourage crystallization of the γ polymorph beyond that caused by the extrusion. These additives may act as nucleation sites, thereby increasing the rate of crystallization of the γ form. In another PA6 composite system, poly(*p*-phenylene terephthalamide) (PPTA) has been shown to act as a nucleation site for and to accelerate the crystallization of α-PA6 in materials made by adding 12-μm PPTA fibers to PA6.[20] The formation of the γ crystallites may also be enhanced by changes in shearing stresses during the extrusion process that are caused by the dissimilar components.

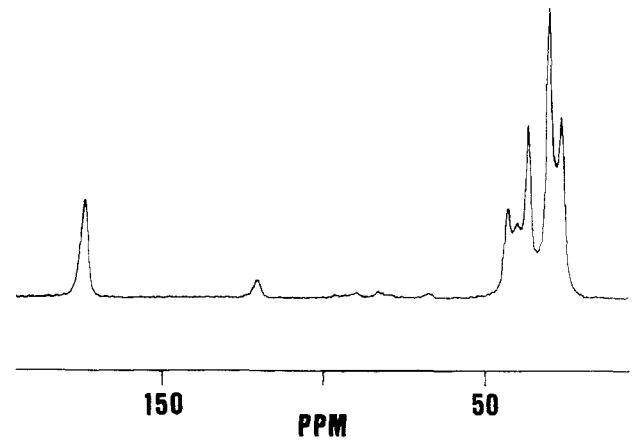

Figure 3. ^{13}C CP/MAS spectrum of sample 5 after 1.5 years of aging under ambient conditions. When compared with Figure 1e, the relative intensity at 40 ppm is lower, indicating a loss of γ crystallites.

As mentioned above, the CP/MAS spectra contain contributions from both the amorphous and crystalline components. The subtraction of the amorphous spectrum from the CP/MAS spectrum effectively deconvolutes the two contributions and gives the spectrum of the rigid components. This is demonstrated in Figure 4 for samples 1 and 4. The new peaks due to the γ structure are clearly visible when the composite difference spectrum, Figure 4f, is compared with the PA6 difference spectrum, Figure 4c. The relative amounts of crystalline and amorphous fractions are needed to calculate these difference spectra. This ratio may be estimated by using the preexponential factors from the double-exponential function used to fit the spin–lattice relaxation data. However, since the T_1 values for the different carbons in the amorphous fraction differ from one another and only one recycle time (1 s) was used to collect the data for the spectra of the amorphous fraction, not all peaks in the spectra collected with 90° pulses are quantitatively represented. Therefore, an apparent inconsistency between the crystalline peak height ratios $C1(\alpha)/C1(\gamma)$ and $C5(\alpha)/C5(\gamma)$ is introduced. This discrepancy is enhanced by the facts that in the first case, C1, the amorphous line at 40 ppm overlaps the line from the γ polymorph and in the second case, C5, the amorphous line at 37 ppm overlaps with the crystalline line from the α polymorph. The result is that rather than an equality, $C1(\alpha)/C1(\gamma) = C5(\alpha)/C5(\gamma)$, an apparent ine-

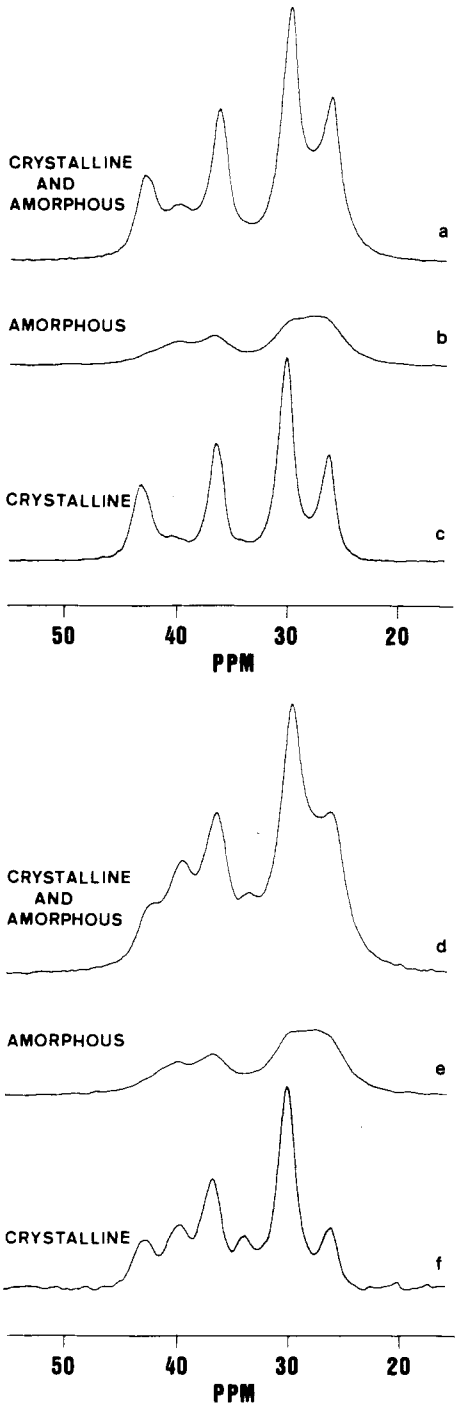

Figure 4. ^{13}C spectra of the aliphatic regions of samples 1 and 4. The CP/MAS spectra are the same as those shown in Figure 1 and contain contributions from both the amorphous and crystalline fractions. The amorphous spectra are measured with a 1-s recycle time and no cross polarization. The difference spectra indicate the appearance of the spectra of the crystalline fractions: (a) sample 1, amorphous plus crystalline fraction (CP/MAS); (b) sample 1, amorphous fraction (MAS); (c) sample 1, crystalline fraction (difference, a – b); (d) sample 4, amorphous plus crystalline fractions (CP/MAS); (e) sample 4, amorphous fraction (MAS); (f) sample 4, crystalline fraction (difference, d – e).

quality $C1(\alpha)/C1(\gamma) < C5(\alpha)/C5(\gamma)$, is observed.

Comparison of the values of the preexponential factors for the crystalline α-PA6 peaks at 43 and 37 ppm with those of the crystalline γ-PA6 at 40 and 34 ppm and assuming equal line widths and cross polarization rates for each type of carbon give the approximate amounts of the α and γ forms in the crystalline fractions of these samples. Sample 1 was found to contain 15% γ-PA6 and samples

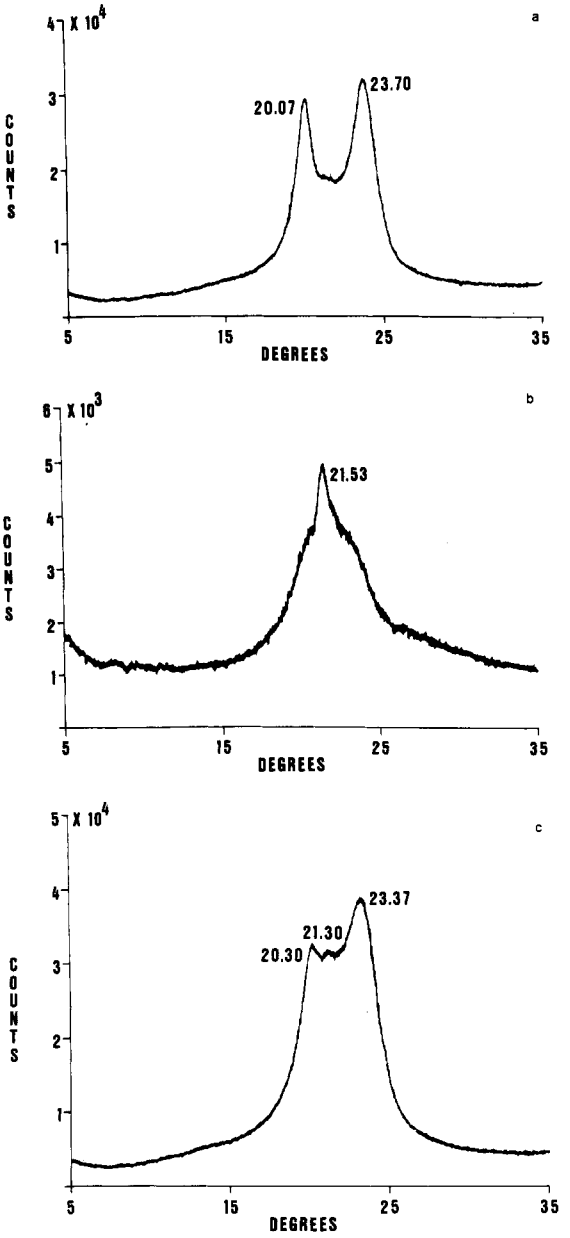

Figure 5. Central portion of the WAXS diffraction patterns: (a) sample 1, original PA6 after 3 years of aging; (b) sample 4, PA6 composite containing prefunctionalized glass balls after 3 years of aging; (c) sample 5, PA6 soon after extrusion.

2–5 contained 41%, 42%, 40%, and 24% γ-PA6, respectively, of the total crystalline fraction. After approximately 2 years of aging, the γ-PA6 fraction of sample 5 diminished to approximately 18%.

X-ray Diffraction. The WAXS pattern of fibers containing predominantly α-PA6 gives pronounced peaks at $2\theta = 20.1°$ and 23.7°. The predominantly γ-PA6 fibers give a large peak at $2\theta = 21.5°$.[8] These same structures are apparent in the WAXS patterns of samples 1, 4, and 5, as shown in Figure 5. The qualitative differences in the structure of the PA6 are obvious from the differences in line shapes. For the original PA6, the two α lines are clearly resolved, while for composite 4 and also composites 2 and 3, the γ line seems to be dominant. The extruded-only sample, shown in Figure 5c, was measured soon after extrusion and is an intermediate case showing both α-like and γ-like line shapes. The X-ray patterns for the two fiber samples were analyzed by using the program of ref 8. The predominantly α-PA6 sample was found by X-ray analysis to contain 9% γ-PA6 in the crystalline fraction.

In comparison, deconvolution of the NMR spectrum using Lorentzian lines gave 19% as the amount of γ crystallites. For the second, predominantly γ sample, the X-ray analysis gave 67% γ and the NMR analysis gave 72% γ. The agreement in both cases is reasonable. It is not surprising that the results are not exactly the same because the regions of crystallinity sampled by the two techniques differ. X-ray diffraction samples the order of a crystalline environment over distances of at least 50–100 Å, while for NMR, this distance is not larger than 5–10 Å.

Conclusions

^{13}C NMR enables us to ascertain the presence of α and γ (or γ-like) crystallites and an amorphous phase in PA6 composites. The carbons on either side of the amide group, C1 and C5, are shifted 3 ppm upfield in the γ polymorph relative to the α polymorph. The CP/MAS spectra of the composites are the same as one another, independent of the nature of the additive. Consistent with the NMR data, the X-ray diffraction patterns show that the composition of the crystallites changes considerably: the composites contain more γ-PA6 than the original sample of pure PA6 contains. The location of the additives adjacent to or included in a particular phase cannot be determined. Less than 1% of the polymer is within 5 nm of the balls and so not readily detectable with NMR. Therefore, the disturbances due to the additives that cause the changes in the NMR spectrum must be long range. Extrusion of PA6 without additives induces the formation of γ-PA6; however, these crystallites are not stable over time and gradually revert to the α polymorph.

Acknowledgment. We thank Dr. J. Aerts (AKZO Research Department, Arnhem) for running the X-ray diffraction patterns and Dr. R. Huisman (ENKA Research Department, Arnhem) for the analysis of the X-ray data with their program. The samples were provided by Dr. W. Koetsier (ENKA Research Department, Arnhem). We also thank Dr. H. T. Edzes for the program with which the exponential decays were analyzed.

Registry No. PA6, 25038-54-4; (3-aminopropyl)triethoxysilane, 919-30-2.

References and Notes

(1) Kricheldorf, H. R.; Leppert, E.; Schilling, G. *Makromol. Chem.* **1974**, *175*, 1705.
(2) Kricheldorf, H. R.; Hull, W. E. *J. Polym. Sci., Polym. Chem. Ed.* **1978**, *16*, 2253.
(3) Kricheldorf, H. R. *Makromol. Chem.* **1978**, *179*, 2675.
(4) Egorov, E. A.; Zhizhenkov, V. V. *J. Polym. Sci., Polym. Phys. Ed.* **1982**, *20*, 1089.
(5) Arimoto, H. *J. Polym. Sci., Part A-2* **1964**, 2283.
(6) Holmes, D. R.; Bunn, C. W.; Smith, D. J. *J. Polym. Sci.* **1955**, *17*, 159.
(7) Arimoto, H. J.; Ishbashi, M.; Hirai, M. *J. Polym. Sci., Part A-3* **1965**, 317.
(8) Heuvel, H. M.; Huisman, R. *J. Polym. Sci., Polym. Phys. Ed.* **1981**, *19*, 121.
(9) Heuvel, H. M.; Huisman, R. *J. Appl. Phys. Sci.* **1981**, *26*, 713.
(10) Earl, W. L.; VanderHart, D. L. *J. Magn. Reson.* **1982**, *48*, 35.
(11) Stejskal, E. O.; Schaefer, J. *J. Magn. Reson.* **1975**, *18*, 560.
(12) Grant, D. M.; Paul, E. G. *J. Am. Chem. Soc.* **1964**, *86*, 2684.
(13) Kricheldorf, H. R.; Muller, D. *Macromolecules* **1983**, *16*, 615.
(14) Veeman, W. S.; Menger, E. M. *Bull. Magn. Reson.* **1981**, *2*, 77.
(15) Veeman, W. S.; Menger, E. M.; Ritchey, W.; De Boer, E. *Macromolecules* **1979**, *12*, 924.
(16) Edzes, H. T.; Veeman, W. S. *Polym. Bull.* **1981**, *5*, 255.
(17) Earl, W. L.; VanderHart, D. L. *Macromolecules* **1979**, *12*, 762.
(18) Gomez, M. A.; Cozine, M. H.; Schilling, F. C.; Tonelli, A. E.; Bello, A.; Fatou, F. G. *Macromolecules* **1987**, *20*, 1761.
(19) Illers, K.-H.; Haberkorn, H. *Makromol. Chem.* **1971**, *142*, 31.
(20) Kumamaru, F.; Oono, T.; Kajiyama, T.; Suehiro, K.; Takayanagi, M. *Polym. Compos.* **1983**, *4*, 135.

Tacticity, Sequence Distribution, Anomalous Linkages, and Alkyl Chain Branching in Ethylene–Vinyl Alcohol Copolymers As Studied by ^1H and ^{13}C NMR

Harm Ketels*

Laboratory of Polymer Technology, Eindhoven University of Technology, PO 513, 5600 MB Eindhoven, The Netherlands

Jo Beulen and Geert van der Velden

DSM Research BV, PO 18, 6160 MD Geleen, The Netherlands. *Received October 19, 1987*

ABSTRACT: A careful reexamination of the 200–300-MHz ^1H NMR spectra of ethylene–vinyl alcohol (E–VOH) copolymers has led to a complete assignment (on a triad level) of all observed methine and hydroxyl resonances. Compositional sequence data and configurational sequence placements (tacticity) have been obtained from ^1H and ^{13}C NMR spectra. The limitations of ^1H and ^{13}C NMR methods for the determination of anomalous structures and nonhydrolyzable chain branching are discussed.

1. Introduction

Copolymers and terpolymers of ethylene (E), vinyl acetate (VA), vinyl alcohol (VOH), and vinyl chloride (VC) have considerable commercial importance. Structure–property relationships have been extensively studied by exploiting among other techniques detailed microstructural analysis via NMR methods. In the past, several papers have demonstrated the usefulness of high-resolution ^1H and/or ^{13}C NMR methods in determining composition, sequence distribution, and cotacticity of these copolymers. Detailed microstructural analysis has been carried out for the following copolymers: E–VA,[1,2] E–VOH,[3,4] E–VC,[5,6] VA–VOH,[7,8] and VA–VC.[9,10] Moreover, terpolymers like E–VA–VOH[3] and E–VA–VC[11] have been studied; however, in these cases only quantitative termonomer compositions could be obtained.

Concentrating on the information available for E–VOH copolymers, researchers have obtained compositional sequence distribution from either ^1H or ^{13}C NMR data of the compositional VOH-centered methine triads (^1H NMR)[3] or alternatively via studies of the compositional methylene diads (^{13}C NMR).[4] Configurationally (i.e.,

0024-9297/88/2221-2032$01.50/0